A numerical and experimental study of natural convective heat transfer from two-sided circular and square horizontal plates having a finite thickness

Rafiq Manna *, Patrick H. Oosthuizen

Queen's University, Kingston, Ontario, Canada K7L 3N6

* Corresponding author, Email: 15rmm1@queensu.ca, ORCID: 0000-0002-8721-6415

Abstract

Several numerical and experimental studies of natural convective heat transfer from two-sided heated horizontal plates are available. In the numerical studies it has usually been assumed that the plate is thin, effectively having no thickness, whereas plates of finite thickness have been used in the experimental studies. The main aim of the present study is to determine whether the plate thickness has a significant influence on the heat transfer rates from the plate surfaces. The effect of the vertical side surface thermal boundary condition and the effect of the plate shape on the heat transfer rates have been also studied. Heat transfer results have, therefore, been numerically obtained for circular and square plates having various thicknesses. The upper and lower plate surfaces have been assumed to be isothermal and at the same temperature. Both the cases where the vertical side surface of the plate is isothermal and at the same temperature as the upper and lower plate surfaces and the case where this vertical side surface is adiabatic have been considered. The solution has been obtained using ANSYS FLUENT©. Variations of the mean Nusselt number with Rayleigh number for various dimensionless plate thicknesses for the two vertical side surface conditions have been obtained for both plates. To validate the numerical results, a limited range of experiments has been undertaken for both shapes. Mean heat transfer rates have been obtained using the lumped capacity method. Results have only been obtained for the case where the plates are exposed to air.

Acknowledgment This work was supported by the Natural Sciences and Engineering Research Council of Canada (NSERC) through its Discovery Grant Program (Grant RGPIN-2015-06444).

List of symbols

A_{plate}	area of the top surface of plate and of bottom surface of plate (m^2)
A_{side}	area of the vertical side surface of plate (m^2)
A_{total}	sum of the areas of the heated surfaces of plate (m^2)
c	specific heat of material from which plate is made (J/kg K)
d	diameter of circular plate (m)
g	gravitational acceleration (m/s^2)
h	thickness of plate (m)
h_t	total heat transfer coefficient (W/m^2 K)
h_r	radiant heat transfer coefficient (W/m^2 K)
h_c	convective heat transfer coefficient (W/m^2 K)
H	dimensionless thickness of plate, h/l (-)
k	thermal conductivity (W/m K)
l	length scale of plate, i.e., d or w (m)
m	mass of plate (kg)
Nu	mean Nusselt number (-)
Nu_{total}	mean Nusselt number based on the mean heat transfer rate per unit area over heated surfaces of plate (-)
Nu_{top}	mean Nusselt number based on the mean heat transfer rate per unit area over upper surface of plate (-)
Nu_{bot}	mean Nusselt number based on the mean heat transfer rate per unit area over lower surface of plate (-)
Nu_{side}	mean Nusselt number based on the mean heat transfer rate per unit area over vertical side surface of plate (-)
P	perimeter of surface (m)
Pr	Prandtl number (-)
$\overline{Q'}$	total heat transfer rate from the heated surfaces of plate (W)
$\overline{Q'}_{top}$	total heat transfer rate from the upper surface of plate (W)
$\overline{Q'}_{bot}$	total heat transfer rate from the lower surface of plate (W)
$\overline{Q'}_{side}$	total heat transfer rate from the vertical side surface of plate (W)
r	radius of circular plate (m)
Ra	Rayleigh number (-)
t	time (s)
T_w	temperature of heated surfaces of plate (K)
T_f	temperature of fluid far from plate (K)
T_i	initial temperature of plate (K)

T_e final temperature of plate (K)
T_m mean temperature of plate (K)
T_s temperature of the surroundings to which plate is radiating (K)
w side length of square plate (m)

Greek Symbols

α thermal diffusivity (m^2/s)
β bulk coefficient of expansion (1/K)
ν kinematic viscosity (m^2/s)
σ Stefan-Boltzmann constant ($W/m^2 K^4$)
ε emissivity of plate (-)

1 Introduction

Situations involving natural convective heat transfer from horizontal plates where the top, bottom and side surfaces are simultanously heated occur in an engineering practice, for example, in the cooling of electrical and electronic components. A limited number of numerical and analytical studies [1, 3, 4, 8, 11, 12] and experimental studies [13, 14] of natural convective heat transfer from two-sided horizontal plates are available. All studies consider air as a fluid except Corcione et al. [8] who studied other fluids beside air.

Chambers and Lee [1] conducted a numerical simulation to determine the local and average natural convection Nusselt numbers for uniformly heated horizontal thin plates with heat being transferred from both upper and lower surfaces simultaneously. Several plate widths with a fixed plate thickness were used. The simulation results were compared with the experimental data obtained by Sparrow and Carlson [2] for the case of upward-facing uniformly heated surface. An excellent agreement was found between the results. The range of Rayleigh numbers used was from 86 to 1.9×10^8. Correlations for the Nusselt number over the range of Rayleigh numbers considered were proposed. Wei et al. [3] undertook a numerical study of the simultaneous natural convective heat transfer from the upper and lower surfaces of a uniformly heated thin plate set at arbitrary inclination angles (0-90°) from horizontal. The plate thickness was fixed at 1/51 of the plate width which was varied. The average Nusselt number correlations for the upper and lower surfaces have been proposed. The values of Rayleigh number used were from 4.8×10^6 to 1.87×10^8. For validation purposes, the results for the horizontally upward-facing uniformly heated plate were compared with the correlation equation of Chambers and Lee [1] as well as with the experimental results of Sparrow and Carlson [2] and good agreement was obtained. Wei et al. [4] numerically investigated the simultaneous natural convective heat transfer above and below an isothermal horizontal thin plate in an infinite space. The plate widths were varied while the plate thickness was set at a fixed value which is 1/51 of the plate width. The range of Rayleigh numbers was from 1.0×10^5 to 1.7×10^7. The results for the upward-facing horizontal surface were compared with the results given by the analytical solution obtained by Pera and Gebhart [5] and with the experimental data of Sparrow and Carlson [2] and for the downward-facing horizontal surface, the results were compared with the numerical calculation of Friedrich and Angirasa [6] and the experimental data of Aihara et al. [7] and a good agreement was obtained for both surfaces. Corcione et al. [8] numerically studied the steady, laminar natural convective heat transfer from an inclined two-sided isothermal plate immersed in different fluids and whose sides are simultaneously heated to the same uniform temperature. For this case, the plate thickness was fixed at 1/50 of the plate length. The range of inclination angles considered was from 0° to 75° (measured from the vertical). The range of Rayleigh numbers was from 10 to 10^7 and the range of Prandtl numbers was from 0.7 to 140. Correlations for the average Nusselt numbers were developed. For validation purposes, the average Nusselt numbers for the vertical orientation at different values of Rayleigh and Prandtl numbers considered were compared with the theoretical solution given by Churchill and Chu [9] for the single-sided heated plate and by Hassan and Mohamed [10] for the two-sided heated plate. A good agreement was found between the results. Fontana [11] conducted a numerical study to predict the influence of the Prandtl number on natural convective heat transfer from an isothermal horizontal infinite thin strip with zero thickness. The Prandtl number values of 0.71, 2.6, 6.7 and 13.5 and the Rayleigh number values of between 10^2 and 10^6 were considered. The results of this study were compared with the results obtained by Wei et al. [4] for the case when the Prandtl number is equal to 0.71 which is effectively the value for air and well agreement was obtained. Correlation equations for the Nusselt number in terms of the Rayleigh and Prandtl numbers were developed. More recently, a numerical study of the simultaneous natural convective heat transfer from the upper and lower surfaces of a thin (no thickness) isothermal horizontal circular plate with inner adiabatic section whose dimensionless diameter was varied to investigate its effect on the heat transfer rate was undertaken by Oosthuizen and Kalendar [12]. The range of conditions included laminar, transitional and fully-turbulent flows. The results obtained in this study were compared with the experimental results of Hassani and Hollands [13] and with the experimental

correlation of Kobus and Wedekind [14] for the laminar flow region. A good agreement was found between the results.

Hassani and Hollands [13] performed experiments to measure natural convective heat transfer from two-sided isothermal plates of different shapes oriented in various directions over a range of Rayleigh numbers from 10 to 10^8. The square and circular plates considered in the study had a dimensionless thickness of only 0.1. A characteristic length has been proposed such that the experimental data obtained could be collapsed with certain other geometrical shapes for a limited range of Rayleigh numbers aiming to generate a universal correlation. Finally, Kobus and Wedekind [14] reported the experimental data of natural convective heat transfer from horizontal isothermal two-sided circular disks of different thickness-to-diameter ratios ranging from 0.063 to 0.163. Dimensionless correlations for Nusselt number over a Rayleigh numbers range from 3×10^2 to 3×10^7 were developed.

The review of the literature has revealed that the existing numerical and experimental studies in this area have mainly dealt with situations in which either the flow over the plate remains laminar, the thickness of the plate remains unchanged (in these studies, either a single value of plate dimensionless thickness was used, see[13] or various values of plate dimensionless thickness were used by either varying the plate width/length while the plate thickness was kept fixed, see [1, 3, 4, 8] or by varying both the plate diameter and thickness at each dimensionless thickness considered, see [14]), or the plate has no thickness, see[11, 12]. To the best knowledge of the authors, there do not appear any detailed study in the literature for predicting the influence of the plate thickness on the natural convective heat transfer from two-sided horizontal plates when the conditions considered are such that laminar, transitional, and turbulent flow over the plate can occur. Such is the main objective of the present research where the various dimensionless plate thicknesses used were obtained by varying the plate thickness while the plate side length/diameter was kept fixed. In addition, the effect of the vertical side surface thermal boundary condition on the heat transfer rates from the plate surfaces for the situations described in the present research have not been studied in detail. Also, there was a lack of knowledge in the literature about the effect of the plate shape on the heat transfer rate, a length scale, $l = 4A_{plate}/P$, has, therefore, been proposed to investigate whether if Nusselt and Rayleigh numbers based on this length scale were used the Nusselt-Rayleigh numbers correlation would be the same for all element shapes considered.

This paper discusses a numerical study of natural convective heat transfer from horizontal two-sided circular and square plates having a finite thickness (see Fig. 1). A limited range of experiments have been undertaken for both shapes to validate the numerical results obtained. Attention will first be given to the numerical part and the experimental part will be explained after.

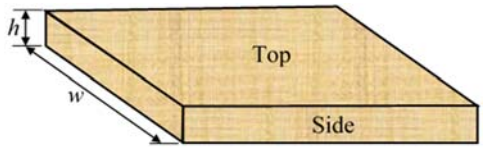

Fig. 1 Finite thickness plate situation considered, a square plate being shown. Also shown are the definitions of the plate thickness, h, and of the top (upper) and of the vertical side surface of a two-sided plate. The bottom (lower) surface is below the top surface

The upper and lower surfaces of the plates are isothermal and at the same temperature which is higher than that of the surrounding fluid and hence there is heat transfer from both the upper and lower surfaces of both plate. The vertical side surface of the plate considered (Fig. 1) are either adiabatic or isothermal and at the same temperature as the upper and lower surfaces of the plate. As shown in Fig. 2 plates having a circular shape and plates having a square shape have been considered in this study. In general, there is an interaction of the flows over the bottom and top surfaces of the plate. The mean heat transfer rates from the top, bottom, and, when the vertical side surface is isothermal, the vertical side surfaces of the plate have been considered as well as the mean heat transfer rate averaged over all the heated surfaces.

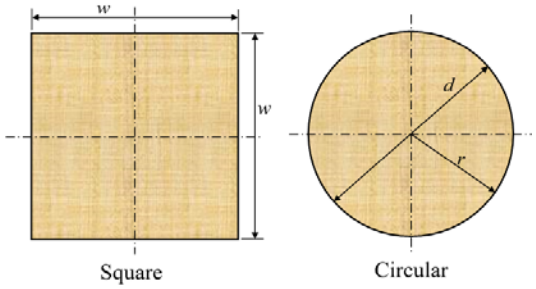

Fig. 2 Square (left) and circular (right) plate shapes considered

Some of the numerical results presented here were included in a paper published in the proceedings of the 3rd Thermal and Fluids Engineering Conference (TFEC) organized by the American Society of

Thermal and Fluids Engineers (ASTFE), Fort Lauderdale, FL, USA, March 4-7, 2018, see [15].

2 Numerical Solution Procedure

The flow has been assumed to be steady and axisymmetric about the vertical center-line in the case of a circular plate and to be symmetric about the two-vertical center planes in the case of a square plate. The fluid properties have been assumed constant except for the density change with temperature which gives rise to the buoyancy forces, i.e., the Boussinesq approach has been adopted. The standard *k*-epsilon turbulence model with buoyancy force effects taken into account has been adopted. This turbulence model has been applied in all calculations and is thus used to determine when transition begins. This approach has been used quite extensively in previous studies, e.g., see [16-22]. The results obtained in the previous studies indicate that while the *k*-epsilon turbulence model does not give good predictions of when transition occurs in all situations it does appear to give results that are of acceptable accuracy for the type of flow situation being considered here.

The solution has been obtained by numerically solving the standard continuity, Navier-Stokes, and energy equations using the commercial CFD solver ANSYS FLUENT©. The following boundary conditions have been considered:

1. All surfaces of the element are isothermal and at the same temperature.
2. Upper and lower surfaces of the element are isothermal and at the same temperature while the vertical side surface is adiabatic (no heat transfer to or from this surface).
3. A uniform pressure condition was assumed on the outer boundaries.

To ensure that the results obtained are grid independent, extensive grid-independence testing using a wide range of grid points and convergence-criteria independence testing was undertaken, and the heat transfer results presented here are grid independent and convergence-criteria independent to better than one per cent. Typical results for mean Nusselt number for various surfaces for each grid test at Rayleigh numbers of 10^7 and 10^{14} for the circular plate which has a dimensionless thickness of 0.3 are shown in Fig. 3. The total number of nodes adopted was 150150.

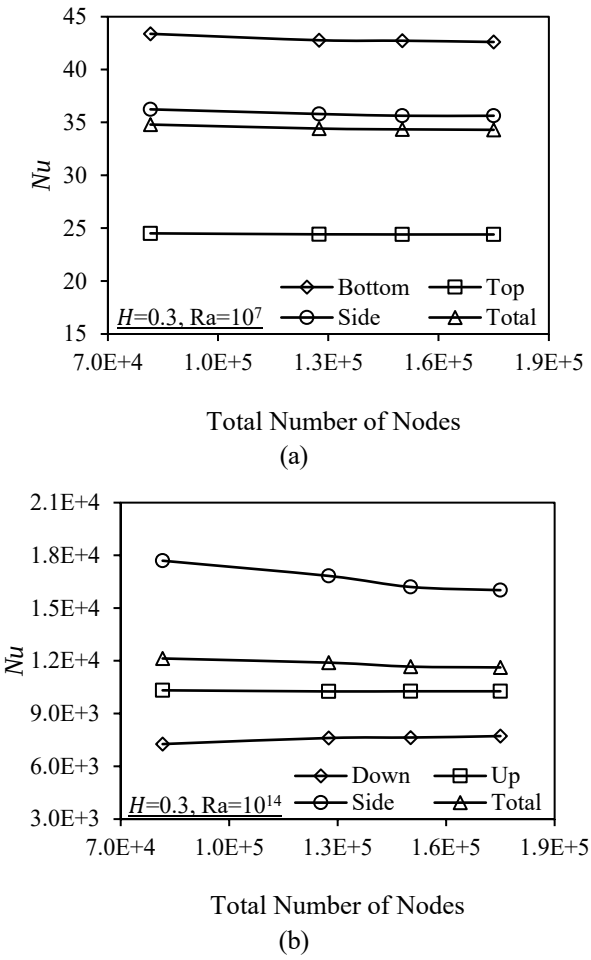

Fig. 3 Effect of grid number on numerical results at: (a) Ra=10^7 and (b) Ra=10^{14} for a circular plate having a dimensionless thickness, *H*, of 0.3

3 Numerical Results

The mean heat transfer rates from the various surfaces of the heated plate have been expressed in terms of the mean Nusselt numbers based on the length scale of the plate defined by, $l = 4A_{plate}/P$, i.e., in terms of the diameter, *d*, in the case of the circular plate and in terms of the side length, *w*, in the case of the square plate, and on the difference between the surface temperature of the plates and the temperature of the undisturbed fluid far from the plate. The mean Nusselt numbers will be dependent on the Rayleigh number, also based on the length scale of the plates and on the difference between the surface temperature of the plate and the fluid temperature far from the plate, and on the Prandtl number. It is often been assumed, e.g., see [24, 25] that for natural convective heat transfer from horizontal heated elements, if the Nusselt and Rayleigh numbers were expressed in terms of the length scale, *l*, defined

above then the variations of Nusselt number with Rayleigh number will be the same for all element shapes. The Rayleigh number is defined by:

$$Ra = \frac{\beta g\, l^3 (T_w - T_f)}{\nu \alpha} \tag{1}$$

Results have only been obtained for a Prandtl number of 0.74, which is effectively the value for air under near standard ambient conditions. The Nusselt numbers will also depend on the dimensionless thickness of the plate, $H = h/l$, and on the thermal boundary condition existing along the vertical side surface of the plate. Mean Nusselt numbers averaged over the upper horizontal surface, over the lower horizontal surface of the plate, averaged over the heated surfaces of the plate, and, in the case of when the plate has isothermal vertical side surface, the mean Nusselt number averaged over the vertical side surface of the plate have been considered. The following Nusselt numbers have therefore been introduced:

$$Nu_{top} = \frac{\overline{Q'}_{top}\, l}{A_{plate}(T_w - T_f)k}, \; Nu_{bot} = \frac{\overline{Q'}_{bot}\, l}{A_{plate}(T_w - T_f)k}$$

$$Nu_{side} = \frac{\overline{Q'}_{side}\, l}{A_{side}(T_w - T_f)k}, \; Nu_{total} = \frac{\overline{Q'}\, l}{A_{total}(T_w - T_f)k} \tag{2}$$

where:

$$\overline{Q'} = \overline{Q'}_{top} + \overline{Q'}_{bot} + \overline{Q'}_{side} \tag{3}$$

and where A_{total}, A_{plate}, and A_{side} are the total area of the heated surfaces of the plate, the areas of the upper and the lower surfaces of the plate, and the area of the vertical side surface of the plate, respectively. Therefore, in the cases where the vertical side surface is adiabatic:

$$A_{total} = 2A_{plate} \tag{4}$$

and $\overline{Q'}_{side} = 0$ while in the cases where the vertical side surface is isothermal:

$$A_{total} = 2A_{plate} + A_{side} \tag{5}$$

From the above equations it follows that when the vertical side surface is adiabatic:

$$Nu_{total} = \frac{Nu_{top} + Nu_{bot}}{2} \tag{6}$$

while when the vertical side surface is isothermal:

$$Nu_{total} = \frac{(Nu_{top} + Nu_{bot})A_{plate} + Nu_{side}A_{side}}{A_{total}} \tag{7}$$

Results for the case where the vertical side surface of the plate is adiabatic will first be considered. Typical variations of the mean Nusselt number averaged over the lower surface of the plate, i.e., Nu_{bot}, over the upper surface of the plate, i.e., Nu_{top}, and over the upper and lower surfaces of the plate, i.e., Nu_{total}, with Rayleigh number for the case of a square plate for two values of the dimensionless plate thickness, H, are shown in Fig. 4 while values of Nu_{bot}, Nu_{top}, Nu_{total} for two value of H for the case of a circular plate are shown in Fig. 5.

It will be seen from these figures that the Nusselt number for the square and circular plates has similar values at the lower Rayleigh number values considered but differ somewhat at the higher Rayleigh number values considered mainly as a result of differences in the predicted Rayleigh number values at which transition to turbulent flow starts to occur with the two plate shapes considered. It will also be seen from these figures that in all cases the Nusselt numbers for the top surface are lower than those for the bottom surface at lower Rayleigh number values but are higher than those for the bottom surface at higher Rayleigh number values.

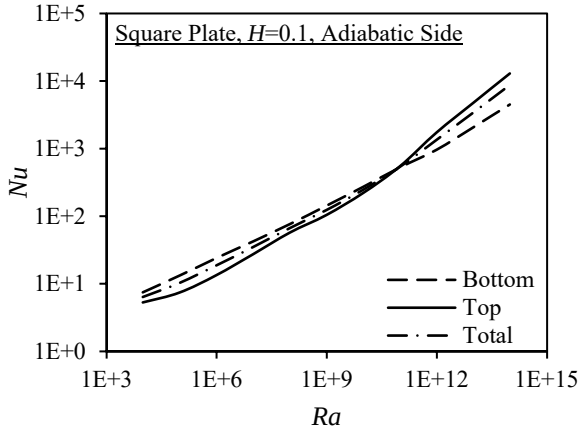

(a)

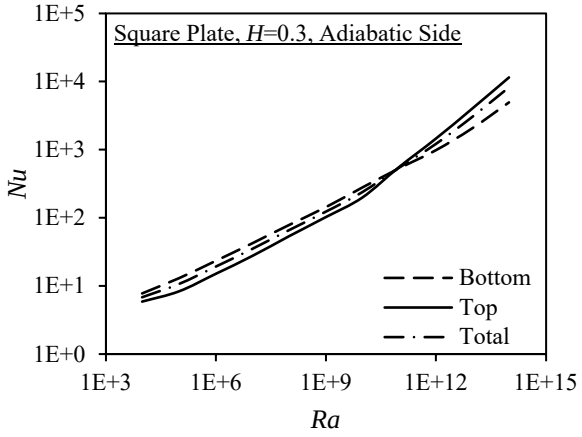

(b)

Fig. 4 Variations of the mean Nusselt numbers for the bottom and top surfaces and for all heated surfaces with Rayleigh number for a square plate having an adiabatic vertical side surface for a dimensionless plate thickness, H, of (a) 0.1 and (b) 0.3

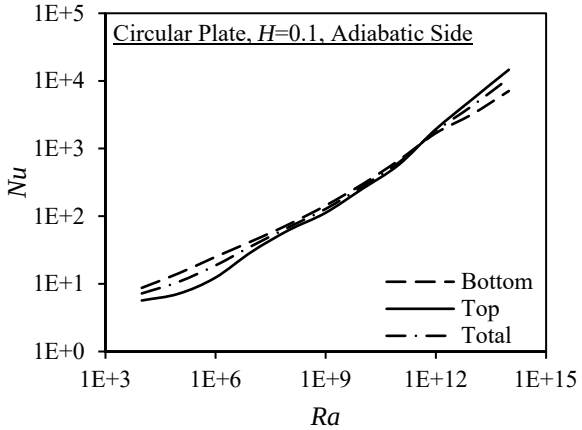

(a)

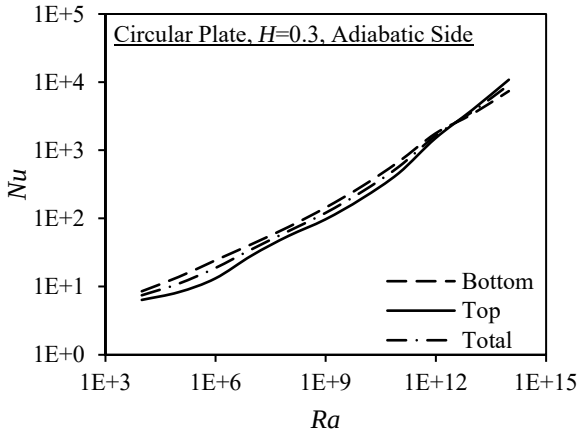

(b)

Fig. 5 Variations of the mean Nusselt numbers for the bottom and top surfaces and for all heated surfaces with Rayleigh number for a circular plate having an adiabatic vertical side surface for a dimensionless plate thickness, H, of (a) 0.1 and (b) 0.3

To further illustrate the effect of the dimensionless plate thickness on the heat transfer rate, variations of the mean Nusselt number with H for various values of the Rayleigh number for the top and the bottom surfaces of a square plate are shown in Fig. 6 and for the top and bottom surfaces of a circular plate are shown in Fig. 7. It can be seen from these figures that the changes in the value of H have an almost negligible effect on the Nusselt numbers for the bottom surface but that the effect of changes in the value of H on the Nusselt numbers for the top surface is significant, the nature of this effect being dependent on the Rayleigh number value.

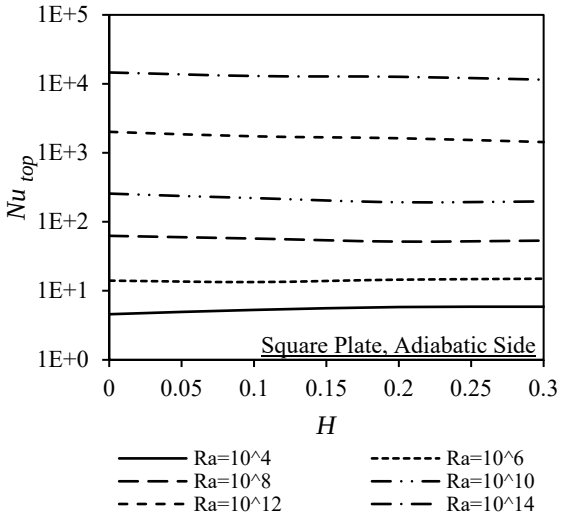

(a)

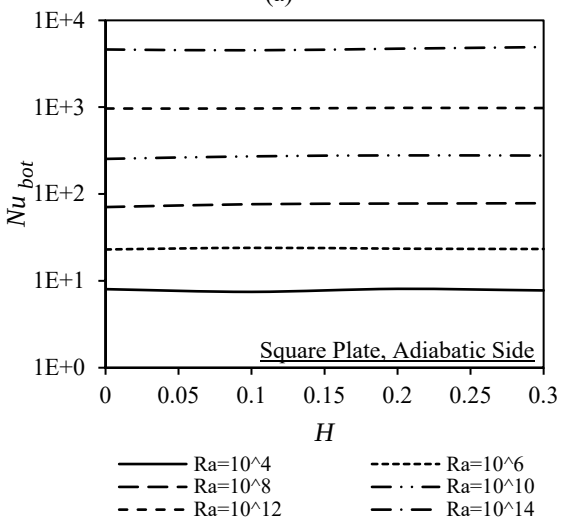

(b)

Fig. 6 Variations of the mean Nusselt number for the (a) top (upper) surface and (b) bottom (lower) surface of a square plate having an adiabatic vertical side surface with dimensionless plate thickness, H, for various values of the Rayleigh number

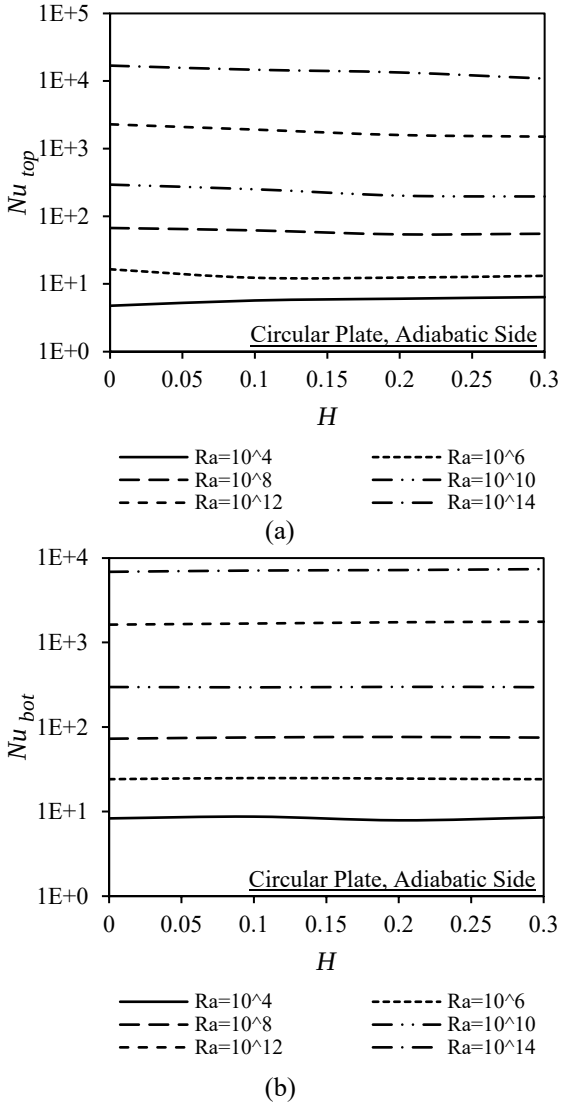

Fig. 7 Variations of the mean Nusselt number for the (a) top (upper) surface and (b) bottom (lower) surface of a circular plate having an adiabatic vertical side surface with dimensionless plate thickness, *H*, for various values of the Rayleigh number

Attention will next be turned to the results for the case where the vertical side surface of the plate is isothermal. Typical variations of the mean Nusselt number averaged over the lower surface of the plate, i.e., Nu_{bot}, over the upper surface of the plate, i.e., Nu_{top}, and over the upper, lower, and vertical side surface of the plate, i.e., Nu_{total}, with Rayleigh number for the case of a square plate for two values of the dimensionless plate thickness, *H*, are shown in Fig. 8 while values of Nu_{bot}, Nu_{top}, Nu_{total} for two values of *H* for the case of a circular plate are shown in Fig. 9. Comparing these results with those for the adiabatic vertical side surface case given in Figs. 4 and 5 shows that the vertical side surface thermal boundary condition has only a very small effect on the Nusselt numbers for the bottom surface but that this vertical side surface thermal boundary condition has a significant effect on the Nusselt numbers for the top surface at the lower Rayleigh number values considered. As with the results for the adiabatic vertical side surface case it will be seen from Figs. 8 and 9 that the results for the square and circular plates have similar values at lower Rayleigh number values considered but differ somewhat at the higher Rayleigh number values. Also, as with the results for the adiabatic vertical side surface case, it will also be seen from these figures that in all cases the Nusselt numbers for the top surface are lower than those for the bottom surface at lower Rayleigh number values but are higher than those for the bottom surface at higher Rayleigh number values considered.

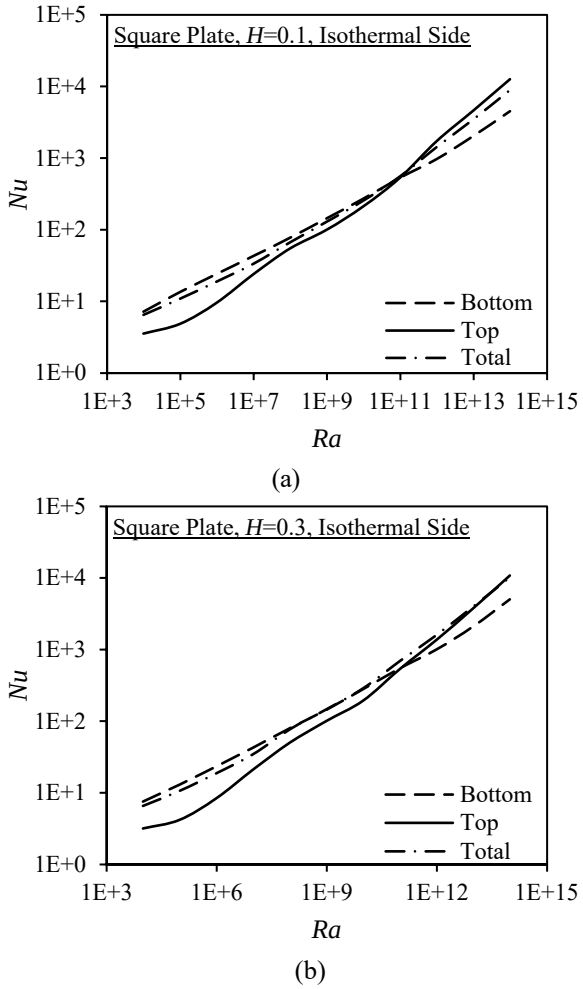

Fig. 8 Variations of the mean Nusselt numbers for the bottom and top surfaces and for all heated surfaces with Rayleigh number for a square plate having an isothermal vertical side surface for a dimensionless plate thickness, *H*, of (a) 0.1 and (b) 0.3

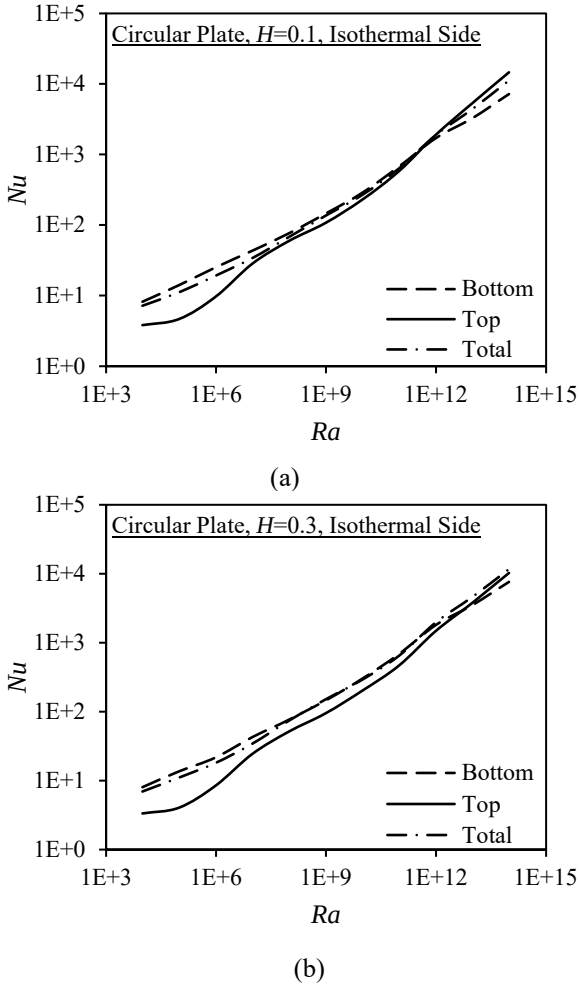

Fig. 9 Variations of the mean Nusselt numbers for the bottom and top surfaces and for all heated surfaces with Rayleigh number for a circular plate having an isothermal vertical side surface for a dimensionless plate thickness, H, of (a) 0.1 and (b) 0.3

Again, to illustrate the effect of the dimensionless plate thickness on the heat transfer rate, variations of the mean Nusselt number with H for various values of the Rayleigh number for the top and the bottom surfaces of a square plate are shown in Fig. 10 and for the top and bottom surfaces of a circular plate are shown in Fig. 11.

As was the case with the adiabatic vertical side surface condition it will be seen from these figures that the changes in the value of H have an almost negligible effect on the Nusselt numbers for the bottom surface but that the effect of changes in the value of H on the Nusselt numbers for the top surface is significant, the nature of this effect again being dependent on the Rayleigh number value. Comparing the results for the isothermal vertical side surface case given in Figs. 10 and 11 with the corresponding results for the adiabatic vertical side surface case given in Figs. 6 and 7 shows that the Nusselt numbers for the bottom surface are essentially the same for the two vertical side surface thermal boundary conditions considered whereas at the lower values of Rayleigh number considered (approximately less than 10^7) the vertical side surface thermal boundary conditions have a significant effect on the Nusselt numbers for the top surface.

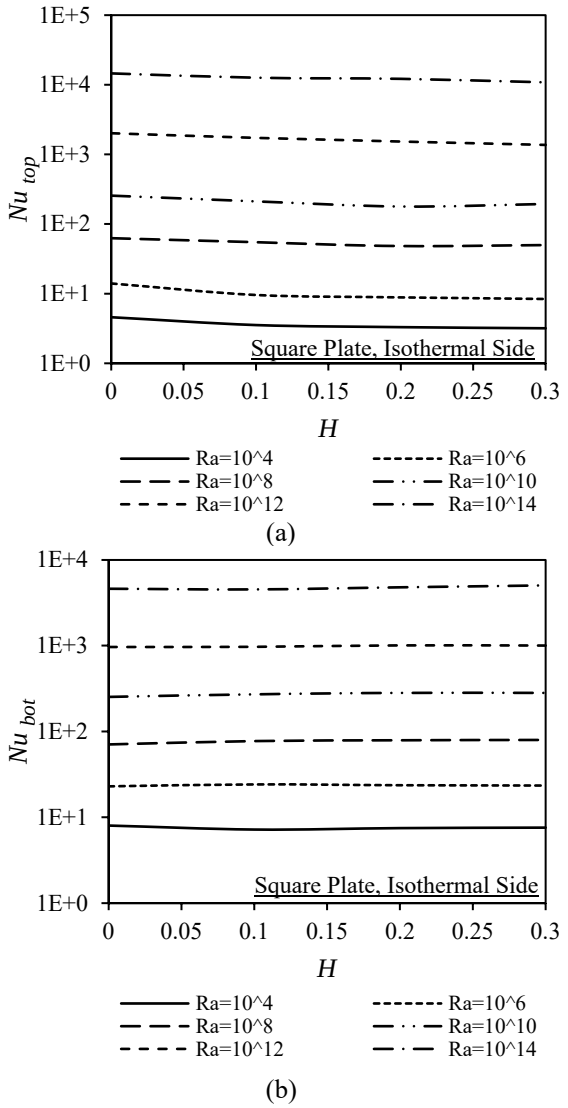

Fig. 10 Variations of the mean Nusselt number for the (a) top (upper) surface and (b) bottom (lower) surface of a square plate having an isothermal vertical side surface with dimensionless plate thickness, H, for various values of the Rayleigh number

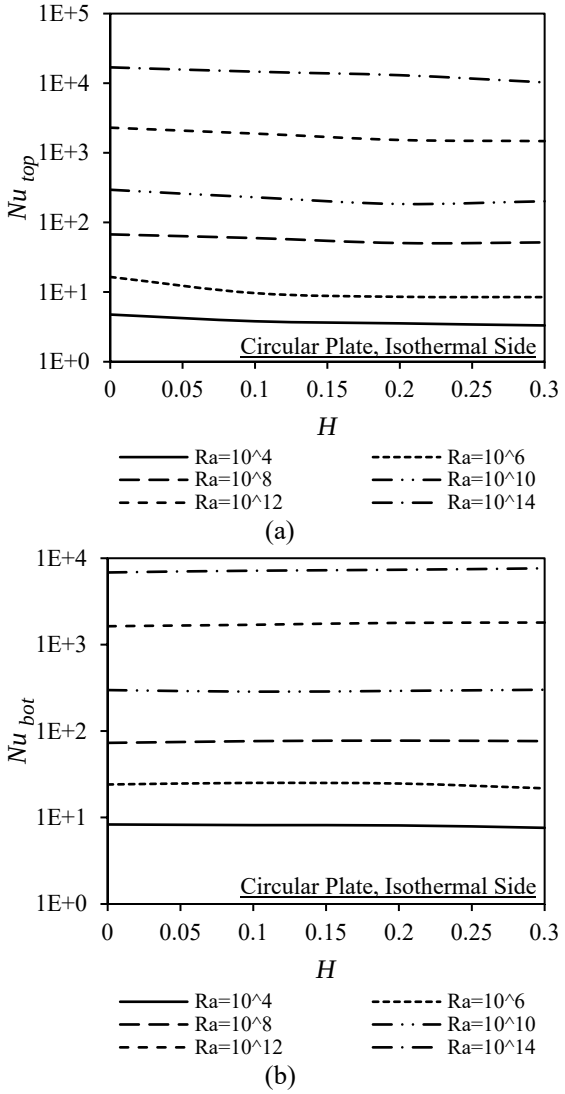

Fig. 11 Variations of the mean Nusselt number for the (a) top (upper) surface and (b) bottom (lower) surface of a circular plate having an isothermal vertical side surface with dimensionless plate thickness, H, for various values of the Rayleigh number

Attention will next be given to the heat transfer from the vertical side surface when it is isothermal. Variations of the mean Nusselt number for this surface with Rayleigh number for the square plate and for the circular plate cases for three values of H are shown in Fig. 12. It will be seen from this figure that the variations for the square and circular plates are very similar and that the effect of the H value on the vertical side surface Nusselt number at a particular value of Ra is relatively small except for H values near 0.1.

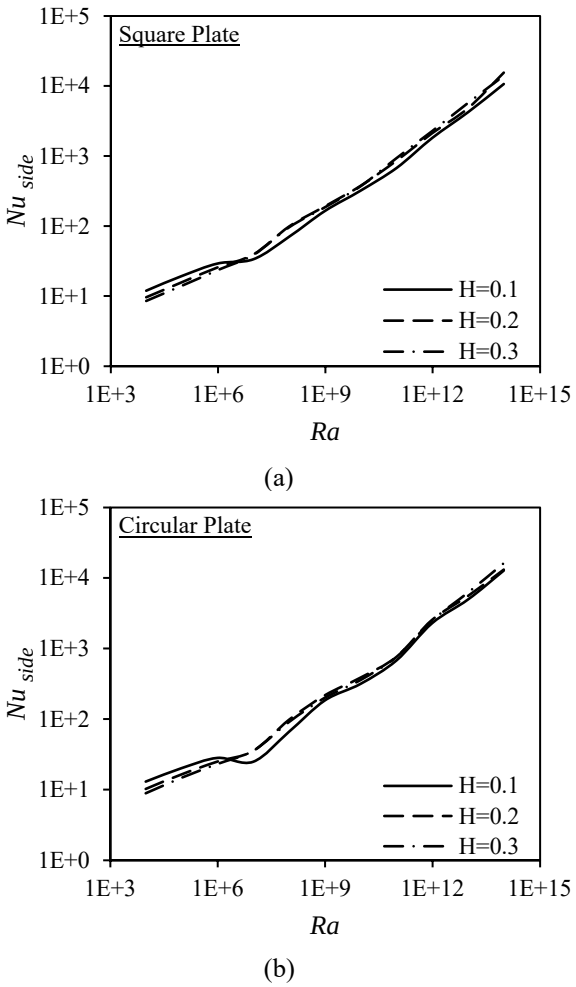

Fig. 12 Variations of the mean Nusselt number for vertical side surface with Rayleigh number for a (a) square plate and (b) circular plate having an isothermal vertical side surface for dimensionless plate thicknesses, H, of 0.1, 0.2, and 0.3

To further illustrate the effect of the vertical side surface thermal boundary condition on the heat transfer rate, typical variations of the mean Nusselt number with Rayleigh number for dimensionless plate thickness, H, of 0.1 for the top and bottom surfaces of a square plate are shown in Fig. 13 and for the top and bottom surfaces of a circular plate are shown in Fig. 14. It can be seen from these figures that as previously explained the effect of the vertical side surface thermal boundary condition on the Nusselt numbers for the bottom surface of the square and circular plates is almost negligible whereas this effect is significant for the top surface of the plates at lower values of Rayleigh number.

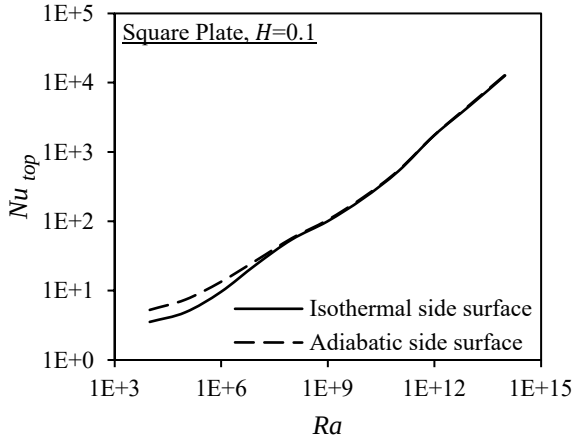

(a)

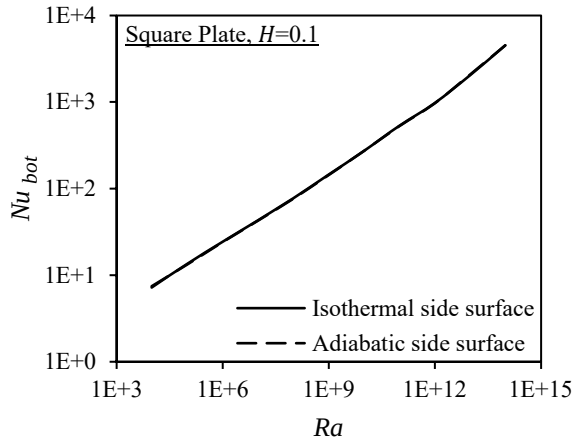

(b)

Fig. 13 Variations of the mean Nusselt number for the (a) top surface and (b) bottom surface with Rayleigh number for a square plate having a dimensionless thickness, H, of 0.1 for the two vertical side surface thermal boundary conditions considered

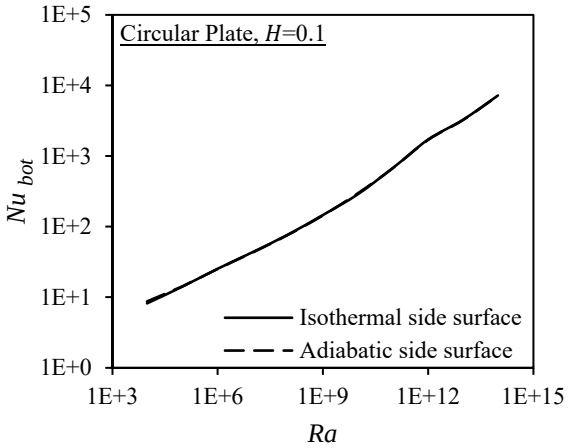

(b)

Fig. 14 Variations of the mean Nusselt number for the (a) top surface and (b) bottom surface with Rayleigh number for a circular plate having a dimensionless thickness, H, of 0.1 for the two vertical side surface thermal boundary conditions considered

Lastly, the effect of the element shape on the heat transfer rate when the length scale, l, is used is shown more clearly by the typical variations of the mean Nusselt number for the top and bottom surfaces with Rayleigh number for the square and circular plates with dimensionless thickness, H, of 0.1 given in Figs. 15 and 16 for the adiabatic and isothermal vertical side surface thermal boundary conditions, respectively. These figures show that for both vertical side surface thermal boundary conditions and over the range of Rayleigh numbers considered the results for the square and circular shapes are in good agreement for the top surface. For the bottom surface, however, the results are in good agreement except at higher values of Rayleigh number.

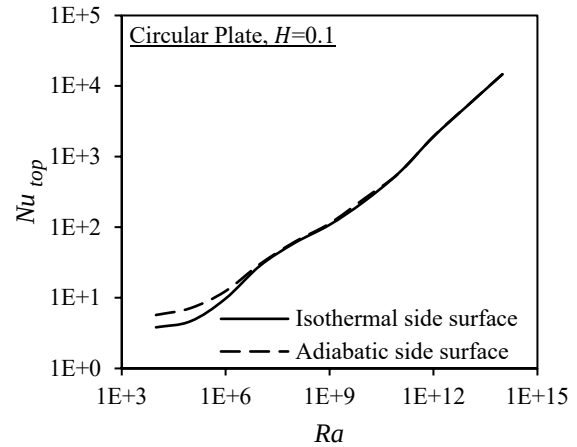

(a)

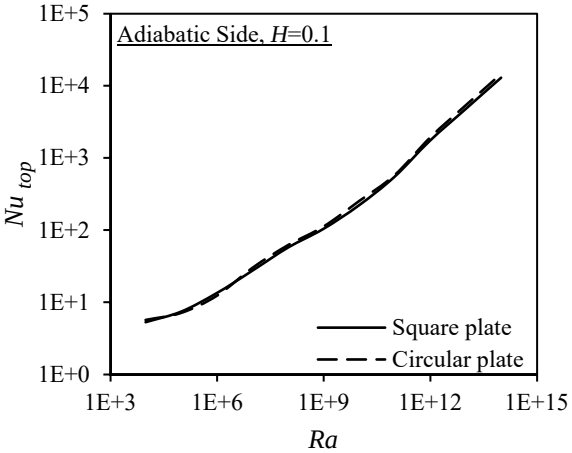

(a)

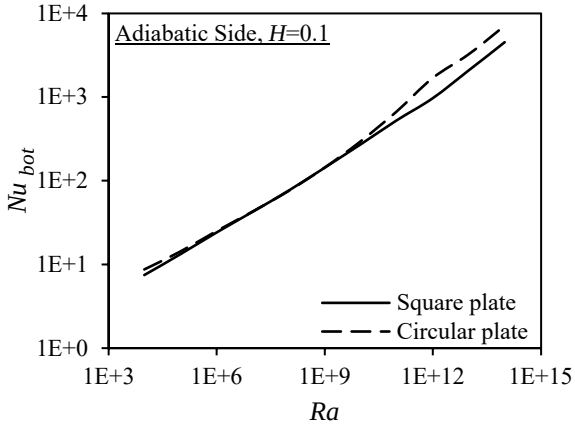

(b)

Fig. 15 Variations of the mean Nusselt number for the (a) top surface and (b) bottom surface with Rayleigh number for square and circular plates having an adiabatic vertical side surface for a dimensionless plate thickness, *H*, of 0.1

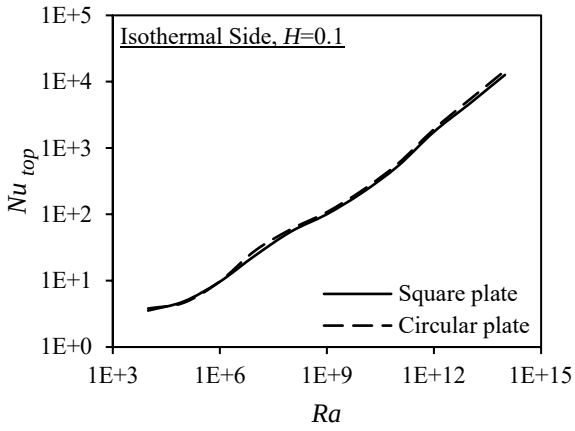

(a)

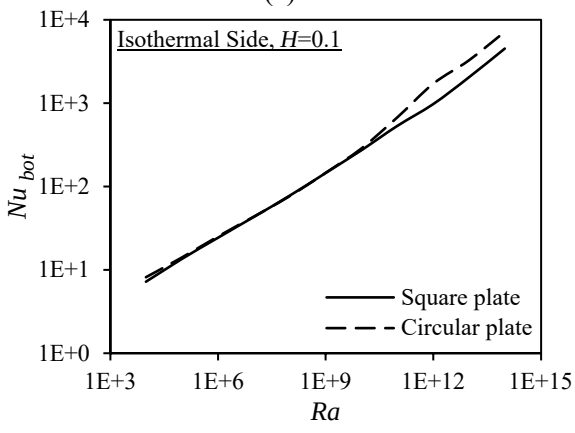

(b)

Fig. 16 Variations of the mean Nusselt number for the (a) top surface and (b) bottom surface with Rayleigh number for square and circular plates having an isothermal vertical side surface for a dimensionless plate thickness, *H*, of 0.1

4 Experimental Apparatus and Procedure

The purpose of the experiments was to validate the numerical results used to predict the natural convective heat transfer from the two-sided square and circular plates. In the experimental study, the mean heat transfer rate from the heated plates considered has been measured using the lumped capacity method.

4.1 Apparatus

To study the natural convective heat transfer from the horizontal plates, a support frame on which the test plates are mounted has been used as shown in Fig. 17. The support frame was constructed using a plexiglas plate on which steel elements with sharp pointy tips were fixed to make the contact with the mounted plates as small as possible. The experiments were conducted in a large test chamber within a laboratory to ensure that its walls do not affect the flow over and the heat transfer from the plates, and to avoid the external disturbances in the room air as well as the temperature changes in the room which may interfere with the flow over the plate while the experiment is taking place. The plates used in the test apparatus were machined from aluminum alloy (Al 6061-$T6$). The dimensions and the mass of the plates are given in Table 1. The plate temperature variation with time has been measured using thermocouples embedded into holes drilled longitudinally into the plates.

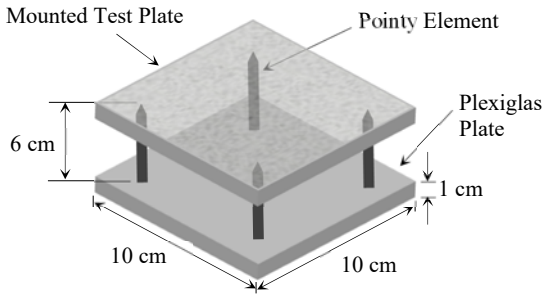

Fig. 17 Schematic representation of the experimental setup. Shown is the square plate mounted on the support frame.

Table 1 Dimensions and mass of the aluminum flat plates

	Flat Plate	
	Square	Circular
Length Scale, l (m)	0.1	0.12
Thickness, h (m)	0.01	0.012
Dimensionless Thickness, h/l	0.1	0.1
Mass, m (kg)	0.27071	0.36676

4.2 Experimental Procedure

As mentioned earlier, the heat transfer rate from the square and circular plates has been measured using the lumped capacity method. Using this method, the plate temperature was raised using an electric oven to roughly 100°C above ambient. The plate was then removed from the oven and exposed to air allowing for cooling to roughly 15°C above ambient. Temperature-time variation as the plate cools has been measured and recorded over the selected temperature range using data acquisition system. It has been assumed that the plate temperature was uniform at any instant of time during cooling process. Therefore, the overall heat transfer coefficient from the plate can be determined from the measured temperature-time variation using the following equation:

$$h_t = \frac{mc}{A_{total}t} ln\left[\frac{(T_i - T_f)}{(T_e - T_f)}\right] \quad (8)$$

To apply the lumped capacity method, it must be assumed that the plate temperature remained uniform at any time instant during the cooling process. Therefore, it is usual to assume that if Biot number, $Bi < 0.1$, the uniform body temperature assumption can be used. For all tests undertaken in the present study, the maximum value of Biot number during the cooling process for each plate was much less than 0.1, which means that the plate temperature remained uniform at any time instant while cooling and as a result, the lumped capacity method was justified to use.

The data was divided into 5-minute intervals. For each interval, $ln\left[\frac{(T_i - T_f)}{(T_e - T_f)}\right]$ was calculated. Using the known value of $\frac{mc}{A_{total}t}$, h_t could be determined.

The value of h_t found using the above procedure was the result of both convective and radiant heat transfer from the plate surfaces to the surrounding air in addition to the conductive heat transfer from the plate to the supporting pointy elements. If the plate can be assumed too small compared with the surroundings to which it is radiating, then it can be assumed that the radiant heat transfer coefficient for each interval is given by the following equation:

$$h_r = \sigma\varepsilon\left(T_m{}^2 + T_s{}^2\right)(T_m + T_s) \quad (9)$$

where, ε is the emissivity of the aluminum plate and it was assumed to equal 0.1 based on the surface finish of the plates considered, T_m is the mean plate temperature during the time interval considered, i.e., $T_m = (T_i + T_e)/2$, and T_s is the temperature of the surroundings to which the plate is radiating. For the situations considered in the present study, $T_s = T_f$. Therefore, equation 9 could be rewritten as:

$$h_r = \sigma\varepsilon\left(\left(\frac{(T_i + T_e)}{2}\right)^2 + T_f{}^2\right)\left(\frac{(T_i + T_e)}{2} + T_f\right) \quad (10)$$

The conductive heat transfer from the plate to the supporting pointy elements is assumed to be negligible due to the very small area of contact between the plate and the pointy elements.

With the radiant heat transfer coefficient estimated, the convective heat transfer coefficient was calculated using the following equation:

$$h_c = h_t - h_r \quad (11)$$

Finally, the Nusselt number, Nu was determined for each interval and hence the variation of Nusselt number with Rayleigh number, Ra could be obtained.

4.3 Uncertainty Analysis

In the experimental study, the uncertainty analysis has been undertaken to refer to a possible value that an error in the measured value may have. To estimate the uncertainty in the experimental values of Nusselt number, the uncertainties in the various variables on which Nusselt number is dependent (uncertainty propagation) have first been estimated. The overall uncertainty in Nusselt number has then been determined using the root-sum-square (RSS) method, see [23]. The relative uncertainty obtained for the experimental values of Nusselt number ranged between 6.7-9.4% for the square plate and between 6.6-9.5% for the circular plate.

5 Experimental Results and Comparison

The experimental results obtained for the square and circular plates were used to examine the validity of the numerical model used. The numerical and experimental heat transfer results have been compared and the variations of the mean Nusselt number with Rayleigh number obtained numerically and experimentally are shown in Figs. 18 and 19 for the square and circular plates, respectively. It can be seen from these figures that the numerical results lie within the experimental error band (the uncertainty of the experimental results explained in the above section) and that the numerical and experimental results compare very closely.

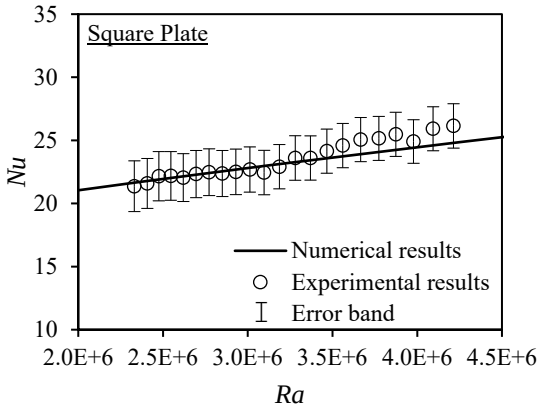

Fig. 18 Comparison between numerical and experimental results for the square plate

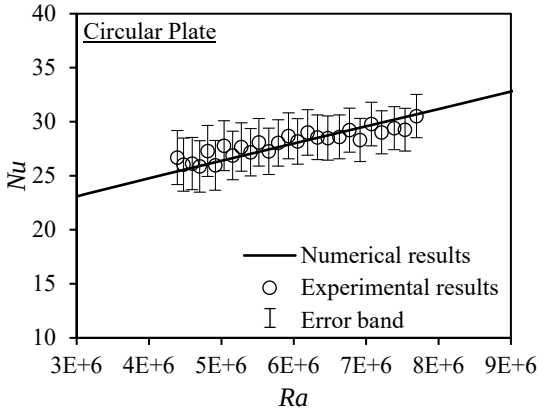

Fig. 19 Comparison between numerical and experimental results for the circular plate

6 Conclusions

The results of the present study show that:

1. In all cases the Nusselt numbers for the top surface are lower than those for the bottom surface at the lower Rayleigh number values considered but are higher than those for the bottom surface at the higher Rayleigh number values considered.
2. Changes in the value of the dimensionless plate thickness, H, have an almost negligible effect on the Nusselt numbers for the bottom surface of the square and circular plates, however, these changes in the value of H have a significant effect for the top surface, the nature of this effect being dependent on the Rayleigh number value being considered.
3. The vertical side surface thermal boundary condition has only a very small effect on the Nusselt numbers for the bottom surface of the square and circular plates but has a significant effect on the Nusselt numbers for the top surface at the lower Rayleigh number values considered.
4. For both vertical side surface thermal boundary conditions, when the length scale, l, is used the variations of Nusselt number with Rayleigh number for the square and circular plates are nearly the same for the top surface of the plates but differ somewhat at the higher Rayleigh number values considered for the bottom surface of the plates mainly as a result of differences in the predicted Rayleigh number values at which transition to turbulent flow starts to occur.
5. In general, the estimated uncertainty in the experimental results was less than 10% and the numerical results lie within the uncertainty of the experimental results. A very good agreement between the present numerical and experimental results was obtained.

Conflict of Interest: The authors declare that they have no conflict of interest.

References

1. Chambers B, Lee TYT (1997) A numerical study of local and average natural convection Nusselt numbers for simultaneous convection above and below a uniformly heated horizontal thin plate. *J. Heat Transfer*, 119(1): 102-108
2. Sparrow EM, Carlson CK (1986) Local and average natural convection Nusselt numbers for a uniformly heated, shrouded or unshrouded horizontal plate. *Int. J. Heat Mass Transfer*, 29(3): 369-379
3. Wei JJ, Yu B, Wang HS, Tao WQ (2002) Numerical study of simultaneous natural convection heat transfer from both surfaces of a uniformly heated thin plate with arbitrary inclination. *J. Heat and Mass Transfer*, 38(4-5): 309-317
4. Wei JJ, Yu B, Kawaguchi Y (2003) Simultaneous natural-convection heat transfer above and below an isothermal horizontal thin plate. *Numer. Heat Transfer Part A*, 44(1): 39-58
5. Pera L, Gebhart B (1973) Natural convection boundary layer flow over horizontal and slightly inclined surfaces. *Int. J. Heat Mass Transfer*, 16(6): 1131-1146.
6. Friedrich MK, Angirasa D (2001) The interaction between stable thermal stratification and convection under a heated horizontal surface facing downward. *Int. J. Non-Linear Mechanics*, 36(5): 719-729
7. Aihara T, Yamada Y, Endo S (1972) Free convection along the downward-facing surface of a heated horizontal plate. *Int. J. Heat Mass Transfer*, 15(12): 2535-2549
8. Corcione M, Habib E, Campo A (2011) Natural convection from inclined plates to gases and liquids when both sides are uniformly heated at the same temperature. *Int. J. Thermal Sciences*, 50(8): 1405-1416
9. Churchill SW, Chu HH (1975) Correlating equations for laminar and turbulent free convection from a vertical plate. *Int. J. Heat Mass Transfer*, 18(11): 1323-1329

10. Hassan KE, Mohamed SA (1970) Natural convection from isothermal flat surfaces. *Int J. Heat Mass Transfer*, 13(12): 1873-1886
11. Fontana L (2014) Free convection heat transfer from an isothermal horizontal thin strip: the influence of the Prandtl number. *J. Thermal Science*, 23(6): 586-592
12. Oosthuizen PH, Kalendar AY (2016) A numerical study of the simultaneous natural convective heat transfer from the upper and lower surfaces of a thin isothermal horizontal circular plate. *Proceedings of the 2016 ASME International Mechanical Engineering Congress and Exposition (IMECE2016)*, Phoenix, Arizona, USA, 8 pages
13. Hassani AV, Hollands KGT (1989) On natural convection heat transfer from three-dimensional bodies of arbitrary shape. *J. Heat Transfer*, 111(2): 363-371
14. Kobus CJ, Wedekind GL (2001) An experimental investigation into natural convection heat transfer from horizontal isothermal circular disks. *Int. J. Heat Mass Transfer*, 44(17): 3381-3384
15. Manna R, Oosthuizen PH (2018) A numerical study of natural convective heat transfer from two-sided circular and square heated horizontal isothermal plates having a finite thickness. *Proceedings of the 3rd Thermal & Fluids Engineering Conferrence (TFEC2018)*, Paper TFEC-21540, Fort Lauderdale, Florrida, USA
16. Savill AM (1993) Evaluating turbulence model predictions of transition. An ERCOFTAC special interest group project, Applied Scientific Research, 51(1-2): 555-562
17. Schmidt RC, Patankar SV (1991) Simulating boundary layer transition with low-Reynolds-number *k-ε* turbulence models: Part 1-an evaluation of prediction characteristics. *J. Turbomachinery,* 113(1): 10-17
18. Plumb OA, Kennedy LA (1977) Application of a *k-e* turbulence model to natural convection from a vertical isothermal surface. *J. Heat Transfer*, 99(1): 79-85
19. Zheng X, Liu C, Liu F, Yang CI (1998) Turbulent transition simulation using the k-ω model. Int. *J. Num. Meth. Eng.*, 42(5): 907-926
20. Albets-Chico X, Oliva A, Perez-Segarra CD (2008) Numerical experiments in turbulent natural convection using two-equation eddy-viscosity models. *J. Heat Transfer*, 130(7): 072501-1-072501-11
21. Xamán J, Álvarez G, Lira L, Estrada C (2005) Numerical study of heat transfer by laminar and turbulent natural convection in tall cavities of Façade elements. *Energy and Buildings*, 37(7): 787-794
22. Kalendar A, Kalendar AY, Alhendal Y (2016) Evaluation of turbulence models for natural and forced convection from flat plates. Computational Thermal Sciences: An International Journal, 8(6): 567-582
23. Kline SJ, McClintock FA (1953) Describing Uncertainties in Single-Sample Experiments. *Mechanical Engineering*, 75(1): 3-8
24. Oosthuizen PH (2015) A numerical study of natural convective heat transfer from horizontal isothermal heated elements of complex shape. *Proceedings of the 1st Thermal & Fluid Engineering Summer Conference (TFESC)*, New York City, USA, 843-854
25. Oosthuizen PH, Kalendar AY (2016) Numerical study of natural convective heat transfer from horizontal heated elements of relatively complex shape having a uniform surface heat flux. *12th International Conference on Heat Transfer, Fluid Mechanics and Thermodynamics (HEFAT2016)*, Costa del Sol, Spain, 1129-1134.